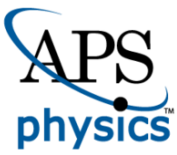

Lateral Line Layout Correlates with the Differential Hydrodynamic Pressure on Swimming Fish

Leif Ristroph, James C. Liao, and Jun Zhang

Phys. Rev. Lett. **114**, 018102 — Published 6 January 2015

DOI: 10.1103/PhysRevLett.114.018102

Lateral line layout correlates with differential hydrodynamic pressure on swimming fish

Leif Ristroph[1], James C. Liao[2], and Jun Zhang[1,3]
[1]*Applied Math Lab, Courant Institute, New York University, New York, New York*
[2]*The Whitney Laboratory for Marine Bioscience, Department of Biology, University of Florida, St. Augustine, Florida and*
[3]*Department of Physics, New York University and NYU-ECNU Institute of Mathematical Sciences at NYU-Shanghai*

The lateral line of fish includes the canal subsystem that detects hydrodynamic pressure gradients and is thought to be important in swimming behaviors such as rheotaxis and prey tracking. Here, we explore the hypothesis that this sensory system is concentrated at locations where changes in pressure are greatest during motion through water. Using high-fidelity models of rainbow trout, we mimic the flows encountered during swimming while measuring pressure with fine spatial and temporal resolution. The variations in pressure for perturbations in body orientation and for disturbances to the incoming stream are seen to correlate with the sensory network. These findings support a view of the lateral line as a 'hydrodynamic antenna' that is configured to retrieve flow signals and also suggest a physical explanation for the nearly universal sensory layout across diverse species.

PACS numbers: Valid PACS appear here

During 500 million years of evolution in water, fishes have diversified into ecosystems worldwide and make up over half of all living vertebrates [1]. Concomitant with their evolutionary success is a refined ability to sense and respond to their fluid environment [2, 3]. A prevalent example of such behavior is rheotaxis, or alignment into a current, a response that is critical to upstream migration and to holding position in a flow [4]. More intricate behaviors include avoiding obstacles [5, 6], reducing swimming effort by slaloming between vortices [7], and localizing and tracking disturbances left by prey [8–10], all of which are possible even in the absence of visual cues. These behaviors suggest that, much more than simply detecting the presence of flow, fish resolve spatial and temporal variations in hydrodynamic signals.

This capability is known to be provided by the lateral line, a specialized sensory system that consists of flow-responsive receptors distributed over the body surface [11, 12]. Previous neurophysiological and physical studies have revealed important insights into the function of individual sensors [13, 14]. Understanding how behavior emerges from sensor-level detection requires additional knowledge about the information available in flows and how such signals are perceived and processed. Thus, dissecting complex swimming behaviors entails identification of the relevant quantity that is sensed, how this quantity is distributed in a given flow, and how the sensory system is laid out along the body to retrieve this information.

Studies into the lateral line have identified two classes of receptors that serve distinct roles [11–14]. Superficial neuromasts are structures that protrude from the skin surface and respond to local flow velocity or shear. Canal neuromasts are recessed within tubes that connect to the outer flow through pores, and these sensors are thought to detect hydrodynamic pressure differences between adjacent pores. Gradients in flow speed along the canal would give rise to such pressure differences. The canal system is especially intriguing, and a long-standing open question is the significance of the strikingly similar canal layout across diverse species [15, 16]. This basic arrangement is well-represented by the rainbow trout (*Oncorhynchus mykiss*) shown in Fig. 1(a). A single branch runs the length of the body trunk and splits into several branches near the head [17]. Thus, the pressure-sensitive subsystem of the lateral line extends over much of the body but is concentrated near the head.

To quantify this observation, we measure how the concentration of canals varies along the body. By taking advantage of anatomical studies that have mapped out the canal system [6, 17–21], we are also able compare the sensory distribution for different species. For a given species, the body is divided into vertical segments, and the number of canal branches crossing each segment is counted. The canal density at each location along the body is computed as the ratio of branches to the segment surface area. This definition, which relies on the canal locations rather than neuromasts or canal pores, uses the most reliable anatomical data available and represents the region of the body for which flow signals can in principle be detected. (See Supplemental Material for a comparison of the density of canals versus canal pores.) In Fig. 1(b), we show the canal density curve for trout (black curve) as well as five other species of ray-finned fishes. All show the same trend of peak concentration near the nose and tapering off to small values beyond 20% of the body length. These species vary in size by two orders of magnitude, occupy a variety of ecological niches, and span the phylogeny of fishes [22], as shown in Fig. 1(c). Thus, although many species exhibit variations such as multiple or absent trunk lines [15, 16], these findings support the view that a basic layout is common to many fishes.

This common layout across diverse fishes has attracted candidate explanations, including a view that the location of canals is morphologically constrained due to

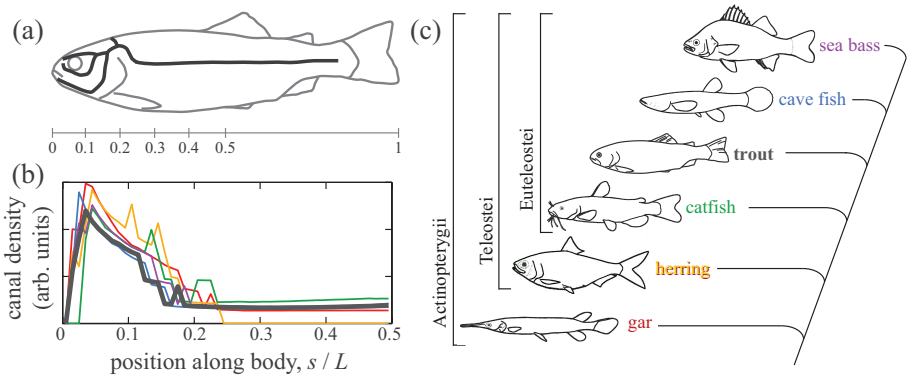

FIG. 1: The lateral line canal system of fishes is concentrated in the head region. (a) Layout of pressure-sensitive canal system for rainbow trout. (b) Number of canals per unit surface area for locations along the body in trout (black curve) and five other species of ray-finned fishes. (c) Phylogeny of fishes for which the canal density is measured.

their association with bones during development [15, 16]. However, variations in the exact placement of canals seem related to the specialized behavior of a species, suggesting a functional role rather than a purely developmental constraint. For example, ventral or dorsal displacement of the trunk canal is common among surface-dwelling and benthic fishes [15, 16]. Further, it has been noted that the head-concentrated system of blind cave fish seems well-suited for detecting obstacles and navigating around complex boundaries [5, 6]. More generally, we propose that the nearly universal canal distribution can be understood through a functional interpretation in which the sensory system layout is related to the hydrodynamic pressure experienced during swimming.

We explore this hypothesis in a simplified but controlled setting that allows us to measure the pressure along the surface of a model rainbow trout. A freshly euthanized trout is first used to produce the high-fidelity hard plastic (polyurethane) model of Fig. 2(a), which replicates the three-dimensional body form down to scale-level details. The model is fixed within the steady laminar flow of a water tunnel [23]. In one method, pressure is recorded directly using electronic transducers that are threaded through holes to meet evenly with the body surface, as shown in Fig. 2(b). A second method involves the measurement of local flow speed along the body, from which the pressure can be inferred by Bernoulli's law. As shown in Fig. 2(c), the flow is seeded with particles and illuminated by a laser sheet, and time-exposed photographs reveal streak-lines whose lengths determine the local flow speed just outside of the boundary layer. These two methods are complementary, with the transducers providing fine time resolution and the Bernoulli method fine spatial resolution.

To validate these methods, we compare their results for the pressure distribution along the model. In Fig. 2(d), we plot the local flow speed U as a function of arc length s along the lateral surface for the model of length $L = 14$ cm aligned with and facing into a flow of speed $U_0 = 48$ cm/s. The flow is slowed to near zero around the stagnation point of the nose and rapidly speeds up to slightly faster than U_0 at locations further along the body. In Fig. 2(e), we show the inferred pressure coefficient using Bernoulli's law [24], $C_p = P/\frac{1}{2}\rho U_0^2 = 1 - (U/U_0)^2$. Here, C_p is a dimensionless measure of pressure, P is the local pressure relative to the far-field, and ρ is the density of water. Bernoulli's law is expected to apply for such a high Reynolds number flow, $\mathrm{Re} = \rho U_0 L/\mu \sim 10^4 - 10^5$, where μ is the viscosity of water. Indeed, the transducer values for the pressure coefficient agree with the Bernoulli measurements. Both indicate that the pressure rapidly drops from its peak value at the nose to near zero at a location just 5% downstream, with smaller changes along the rest of the body.

These measurements correspond to gliding motions, and we also expect that high pressure is anteriorly concentrated during undulatory swimming. Indeed, our pressure distribution is consistent with measurements on swimming fish [6, 25] as well as analytical calculations [26] and computational flow studies [6]. Most importantly, by comparing Fig. 2(e) to 1(b), we find that high pressure is concentrated within a significantly smaller region than the canal density. Thus, the canal distribution does not directly correlate with hydrodynamic pressure.

During complex interactions with flows, it is likely that spatial and temporal *variations* in pressure provide more pertinent information than this steady pressure. To investigate this hypothesis, we determine how the canal layout correlates with pressure changes during biologically-relevant perturbations. Inspired by the robust rheotactic alignment behavior of fish, we first consider the redistribution of pressure associated with changes in yaw orientation of the body relative to the oncoming flow. In Fig. 3(a), we plot the pressure coefficient for the right and left sides when the model is oriented 10° to the left. Overall, the flow-facing (right) side experiences higher pressure than the leeward (left) side, suggesting that the pressure difference across the body could serve as an indication of yaw misalignment [27]. Because the canal system is thought to directly measure local gradients in pressure [13, 14], making use of this information would require integration of this signal along the body and bilateral comparison [28].

In Fig. 3(b), we observe that this right-left pressure differential also increases with yaw angle, thus providing a means for fish to measure orientation relative to the flow. Data for all angles show a similar trend, rising from zero at the nose to a peak within a few percent down the

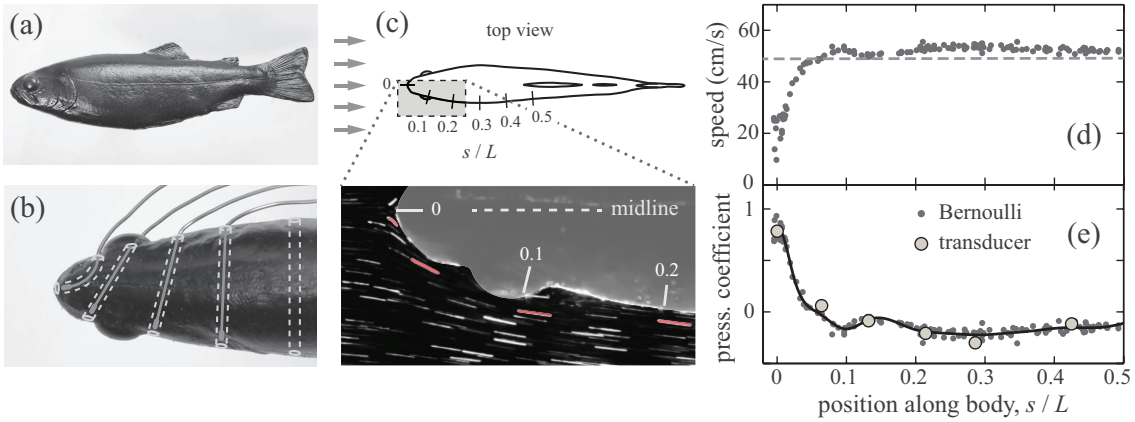

FIG. 2: Hydrodynamic pressure is concentrated at the nose of a swimming fish. (a) A plastic model trout (body length $L = 14$ cm) is cast from a mold and placed in a flow of speed 48 cm/s. (b) Pressure along the lateral side is measured directly by transducers threaded through the model [23]. (c) Photographs of exposure time 1/200 s reveal streak-lines of particles illuminated by a laser sheet. (d) Local flow speed measured from streak-lines for locations along the body and outside the mm-scale boundary layer. (e) Pressure coefficient C_p inferred from speed measurements and Bernoulli's law (dots), as well as by direct measurement using pressure transducers (circles).

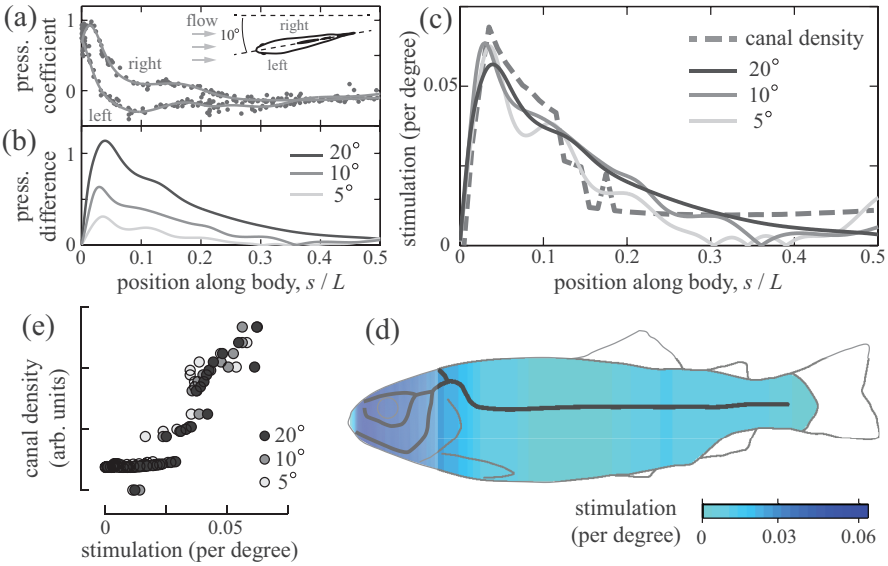

FIG. 3: Canals are concentrated where pressure changes are greatest for a fish oriented at an angle relative to the oncoming flow. (a) Pressure distribution on both sides of a model trout with yaw angle 10°. (b) Pressure differences across the body are amplified for increasing yaw angle. (c) At each location, the *stimulation* is defined to be the change in pressure difference across the body per change in yaw. Stimulation curves are similar for all data sets, and all resemble the canal density distribution. (d) Overlaying stimulation (color map) on a diagram of the trout shows that canals are concentrated at locations where the pressure changes are strongest. (e) Canal density correlates with pressure stimulation.

body and ultimately tapering towards zero. Increasing the angle amplifies the pressure difference at any given location, with a doubling of yaw leading to a doubling of this differential. Such a linear encoding could greatly simplify the neural processing involved in rheotaxis.

Most importantly, these data show that, across all angles, some regions along the fish are consistently subject to stronger changes in pressure. We quantify this by defining the *pressure stimulation* as the derivative of the right-left pressure coefficient difference with respect to yaw angle, ψ. That is, the stimulation as a function of arc length s is given by $\mathrm{d}[C_p^{\mathrm{right}}(s) - C_p^{\mathrm{left}}(s)]/\mathrm{d}\psi$. For an angle of $\psi = 10°$, for example, the stimulation curve can be approximated by dividing the pressure difference curve by 10°. Fig. 3(c) shows that this definition collapses the data sets for all angles. Further, these curves show a remarkable resemblance to the canal density itself, which is plotted as a dashed line in Fig. 3(c). We illustrate this correspondence in Fig. 3(d), where a color map of the stimulation is overlaid on a schematic of the trout and its canal system. Thus, the canals are concentrated where the pressure changes are greatest. To assess this relationship, we plot in Fig. 3(e) the canal density versus pressure stimulation, where each point represents a 1% segment along the fish body. The clear correlation ($R^2 = 0.83$) indicates that the lateral line canals are concentrated at locations of strong hydrodynamic signals, specifically the bilateral pressure difference.

To complement spatial perturbations, we next consider the *temporal* changes associated with a flow disturbance. Motivated by prey detection, we induce a brief disruption to the incoming flow while using transducers to record

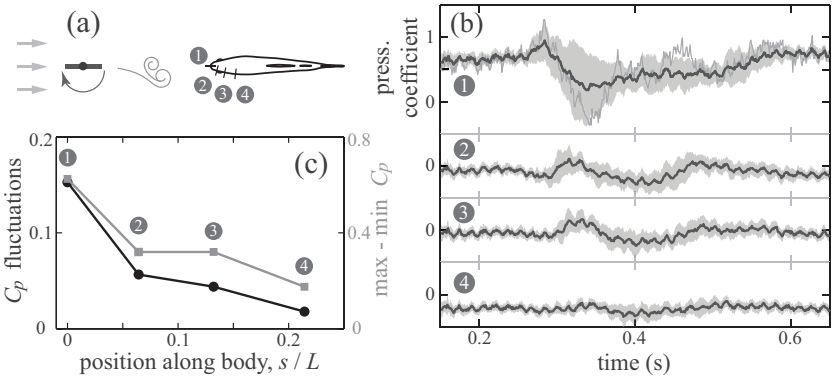

FIG. 4: Pressure fluctuations in response to an induced flow disturbance. (a) The disturbance is generated by an upstream vertical foil that is initially aligned with the flow and rapidly rotates through 180° [23]. (b) Four transducers record the pressure versus time, and the mean (black curve) and standard deviation (gray band) are shown for 20 trials. A sample time trace (thin gray curve) is shown in the top panel. (c) Two measures of pressure fluctuations: The standard deviation averaged throughout the disturbance (black, left axis) and the difference between maximum and minimum values of pressure (gray, right axis).

pressure over time. We fix a vertical plate one body length upstream of the fish model [23]. As indicated in Fig. 4(a), the plate is initially aligned with the flow and is then triggered to rapidly rotate through 180°, returning to the aligned orientation [29]. Thus, this technique provides a strong but transient flow disturbance. Figure 4(b) shows the mean and standard deviation over 20 trials for the pressure coefficient at four locations along the model. We quantify these fluctuations by (1) averaging of the standard deviation of pressure during the perturbation and (2) computing the difference between the maximum and minimum pressures. As shown in Fig. 4(c), both quantities show that fluctuations are strongest at the front and are weaker downstream. Thus, with the exception of the leading few percent at the nose, these pressure changes show a similar distribution along the body as measured for the case of yaw perturbations.

Collectively, our findings suggest that the arrangement of the lateral line system reflects the hydrodynamic information available during swimming. In particular, anatomical measurements and flow experiments show that the canal system is concentrated at locations on the body that experience strong spatial and temporal variations in pressure. Thus, much in the same way that antenna geometries are designed to detect electromagnetic signals, the canal system might be viewed as a 'hydrodynamic antenna' that is laid out on the body surface and configured to detect pressure changes [30]. This view is promising in that it provides an explanation for the highly conserved sensory architecture across many species. Ultimately, it is the slender and streamlined body plan common to these swimmers that leads to an anteriorly-concentrated pressure profile, making the head region particularly sensitive to flow fluctuations.

While we have focused on rheotaxis and prey detection in trout, we expect similar results for other species and for other flow-sensing situations. For example, blind cave fish use the lateral line as a 'distant touch' sense that allows for navigation around boundaries without vision and without direct contact [26]. In an approach to a wall, it has been shown that the pressure distribution is significantly affected only for the leading 20% of the body [6], which is consistent with the region of stimulation observed in our experiments. It is also tantalizing to consider the additional hydrodynamic signals available during body undulations, where pressure variations could be used as feedback to modify swimming motions [11, 31]. Further, as with most biological systems, the common canal layout likely reflects no single function and may offer advantages beyond the correlation of the sensory system with the relevant signals. The branching at the head could be used to gather three-dimensional information, for example, and the head-concentrated layout could also serve to isolate sensation from the self-generated fluctuations associated with caudal propulsion.

More broadly, the diversity of fishes provides an opportunity to test the generality of the correlation reported here on species with variations in canal placement as well as in body shape. Canal variations range from displacement of the trunk line for surface or bottom dwellers to highly ramified head canals for schooling fish, and variations may be linked to swimming behavior and habitat [15, 16]. Similarly, deviations from a streamlined body plan would modify pressure and thus may be accompanied by a modified canal layout. Further, the superficial neuromast subsystem may also be organized according to this principle, in which case these receptors may be distributed according to shear stress [6] or changes in stress. Finally, this idea could serve as a design principle for placing detectors on underwater vehicles [27, 32], where it would offer the advantage of gathering flow information using a relatively sparse sensory network.

We thank O. Akanyeti, S. Childress, N. Moore, A. Libchaber and M. Shelley for discussions. This work was supported by the NSF (DMS-1103876 to LR, IOS-1257150 to JCL), NIH (R01-DC-010809 to JCL), and DOE (DE-FG02-88ER25053 to JZ).

[1] G. Helfman, B. B. Collette, D. E. Facey, and B. W. Bowen, *The diversity of fishes: Biology, evolution, and ecology* (John Wiley & Sons, 2009).

[2] H. Bleckmann, in *The behaviour of teleost fishes* (Springer, 1986), pp. 177–202.

[3] J. C. Liao, Philosophical Transactions of the Royal Society B: Biological Sciences **362**, 1973 (2007).

[4] J. C. Montgomery, C. F. Baker, and A. G. Carton, Nature **389**, 960 (1997).

[5] H. Abdel-Latif, E. Hassan, and C. von Campenhausen, Naturwissenschaften **77**, 237 (1990).

[6] S. P. Windsor, S. E. Norris, S. M. Cameron, G. D. Mallinson, and J. C. Montgomery, The Journal of Experimental Biology **213**, 3819 (2010).

[7] J. C. Liao, D. N. Beal, G. V. Lauder, and M. S. Triantafyllou, Science **302**, 1566 (2003).

[8] J. C. Montgomery and J. A. MacDonald, Science **235**, 195 (1987).

[9] J. Engelmann, W. Hanke, J. Mogdans, and H. Bleckmann, Nature **408**, 51 (2000).

[10] K. Pohlmann, F. W. Grasso, and T. Breithaupt, Proceedings of the National Academy of Sciences **98**, 7371 (2001).

[11] S. Dijkgraaf, Biological Reviews **38**, 51 (1963).

[12] J. Blaxter, Biological Reviews **62**, 471 (1987).

[13] A. Kroese and N. Schellart, Journal of Neurophysiology **68**, 2212 (1992).

[14] S. Coombs and S. Van Netten, Fish physiology **23**, 103 (2006).

[15] S. Coombs, J. Janssen, and J. F. Webb, in *Sensory biology of aquatic animals* (Springer, 1988), pp. 553–593.

[16] J. Webb, Brain, Behavior and Evolution **33**, 34 (1989).

[17] Y. I. Siregar, Acta Zoologica **75**, 213 (1994).

[18] T. W. Bamford, The Annals & Magazine of Natural History **8**, 414 (1941).

[19] J. Song and R. Northcutt, Brain, Behavior and Evolution **37**, 24 (1991).

[20] R. G. Northcutt, P. H. Holmes, and J. S. Albert, Journal of Comparative Neurology **421**, 570 (2000).

[21] J. Diaz, M. Prié-Granié, M. Kentouri, S. Varsamos, and R. Connes, Journal of Fish Biology **62**, 24 (2003).

[22] J. S. Nelson, *Fishes of the World* (John Wiley & Sons, 2006).

[23] Laminar flow is provided by a 6-inch flow visualization water tunnel (Engineering Laboratory Design), and the incoming flow speed is monitored by laser doppler velocimetry (TSI). Pressure is measured with Millar Mikro-Tip transducers of size 1 mm, frequency response 20 kHz, sample rate 100 Hz, and sensitivity 2mV/10V. Transducers are validated using both hydrostatic pressure and dynamic pressure for flow around a sphere. The streakline analysis employs glass microbubbles (3M) as flow tracers and a high resolution camera (Nikon D4). Temporal flow perturbations are provided by a rapid 180° rotation of a thin vertical plate that is 2.5 cm in streamwise length.

[24] D. J. Tritton, Oxford, Clarendon Press, 1988, 536 p. **1** (1988).

[25] A. B. Dubois, G. A. Cavagna, and R. S. Fox, Journal of Experimental Biology **60**, 581 (1974).

[26] E.-S. Hassan, Biological Cybernetics **66**, 443 (1992).

[27] R. Venturelli, O. Akanyeti, F. Visentin, J. Ježov, L. D. Chambers, G. Toming, J. Brown, M. Kruusmaa, W. M. Megill, and P. Fiorini, Bioinspiration & Biomimetics **7**, 036004 (2012).

[28] E. Denton and J. Gray, Philosophical Transactions of the Royal Society of London. Series B: Biological Sciences **341**, 113 (1993).

[29] P. W. Webb, Journal of Experimental Biology **207**, 955 (2004).

[30] J. S. Schwarz, T. Reichenbach, and A. Hudspeth, The Journal of Experimental Biology **214**, 1857 (2011).

[31] K. Yanase, N. A. Herbert, and J. C. Montgomery, The Journal of Experimental Biology **215**, 3944 (2012).

[32] Y. Yang, J. Chen, J. Engel, S. Pandya, N. Chen, C. Tucker, S. Coombs, D. L. Jones, and C. Liu, Proceedings of the National Academy of Sciences **103**, 18891 (2006).